Unimolecular Chemiexcited Oxygenation of Pathogenic Amyloids

Hiroki Umeda,[1] Kayo Suda,[2] Daisuke Yokogawa,[2] Shigehiro A. Kawashima,[1] Harunobu Mitsunuma,[1] Yuki Yamanashi,[1] and Motomu Kanai[1,*]

[1]Laboratory of Synthetic Organic Chemistry, Graduate School of Pharmaceutical Sciences, The University of Tokyo, Tokyo 113-0033, Japan

[2] Laboratory of Theoretical Chemistry, Graduate School of Arts and Sciences, The University of Tokyo, Tokyo 153-8902, Japan

Supporting Information Placeholder

ABSTRACT: Pathogenic protein aggregates, called amyloids, are etiologically relevant to various diseases, including neurodegenerative Alzheimer disease. Catalytic photooxygenation of amyloids, such as amyloid-β (Aβ), reduces their toxicity; however, the requirement for light irradiation may limit its utility in large animals, including humans, due to the low tissue permeability of light. Here, we report that *Cypridina* luciferin analogs, **dmCLA-Cl** and **dmCLA-Br**, promoted selective oxygenation of amyloids through chemiexcitation without external light irradiation. Further structural optimization of **dmCLA-Cl** led to the identification of a derivative with a polar carboxylate functional group and low cellular toxicity: **dmCLA-Cl-acid**. **dmCLA-Cl-acid** promoted oxygenation of Aβ amyloid and reduced its cellular toxicity without photoirradiation. The chemiexcited oxygenation developed in this study may be an effective approach to neutralizing the toxicity of amyloids, which can accumulate deep inside the body, and treating amyloidosis.

Aberrant protein aggregates, amyloids, are related to the etiology of various amyloidoses.[1] There are more than 37 types of amyloidosis, including Alzheimer disease (AD), Parkinson disease (PD), and transthyretin amyloidosis (TTRA). Hallmarks of these amyloidoses are amyloids of amyloid-β (Aβ) and tau protein, α-synuclein (αSyn), and transthyretin (TTR), respectively. Amyloids share a common, characteristic quaternary structure, cross-β sheets, and accumulate either locally (e.g., in the central nervous system for AD and PD) or systemically (for TTRA). Many amyloidoses lack effective therapeutic treatments today. However, reduction of amyloid levels is recognized as an effective treatment, as is exemplified by the recently approved *anti*-AD antibody drug, lecanemab.[2] Identification of small-molecule amyloid modifiers or degraders functionally equivalent to such biologics is an important next step.[3]

Chemical modification of amyloids, especially amyloid-selective photocatalyzed oxygenation (Figure 1A),[4] is an emerging approach to neutralize and degrade amyloids.[5] Although small-molecule photocatalysts successfully oxygenated Aβ amyloid and decreased the amyloid level in AD-model mice,[6] the photooxygenation strategy may be difficult to apply to humans due to the limited permeability of light through tissues.[7] To overcome this hurdle, we envisioned chemiexcitation process to generate an active species capable of oxygenation without photoirradiation. Ran and coworkers developed chemiluminescent probes for fluorescence detection of Aβ amyloid in mice brains.[8] More recently, the same group devised a bimolecular chemiluminescence resonance energy transfer (CRET) system comprised by a chemiluminescent molecule (**ADLumin-4**) and a diazirine-containing ligand molecule for Aβ amyloid (**CRANAD-147**), covalently modifying amyloid with carbene species photolytically generated from **CRANAD-147** by the internal light generated from **ADLumin-4**, and consequently reducing the Aβ level in mice brains (Figure 1B).[9] Here we report single molecular, amyloid-selective chemiexcited oxygenation without relying on external light irradiation (Figure 1C).[10]

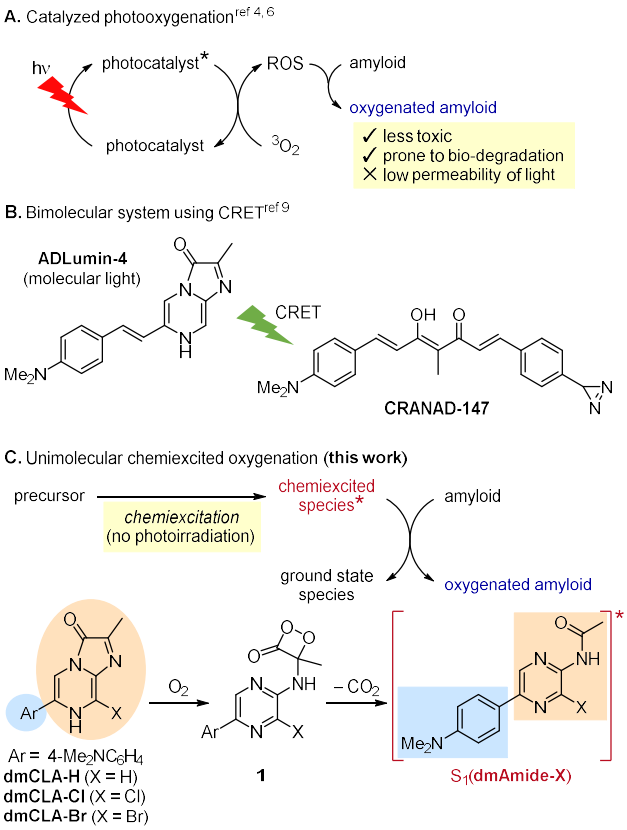

Figure 1. Chemical modifications and degradation of amyloids. **A.** Catalytic photooxygenation converts amyloids to less-toxic oxygenated forms susceptible to degradation by biological mechanisms.[11] However, low tissue permeability of light is a possible hurdle for therapeutic applications. **B.** Chemiluminescence of **ADLumin-4** facilitates carbene formation from **CRANAD-147** binding to Aβ amyloid through CRET, leading to chemical modifications of the amyloid.[9] **C.** This work: autooxidation and decarboxylation of **dmCLA-X** generate excited state species (chemiexcitation). These chemiexcited species selectively oxygenate amyloids without photoirradiation.

We employed the chemiluminescent probe **dmCLA-H**[12] as a lead compound due to its high quantum yield and the structural similarity to a turn-on amyloid-sensing fluorescent probe, thioflavin-T (ThT).[13] **dmCLA-H** converts to an excited singlet state (S_1) of **dmAmide-H** [S_1(**dmAmide-H**)] through two chemical steps: aerobic oxidation affording dioxetanone intermediate **1**, followed by decarboxylation under physiological conditions (Figure 1C).[12] Thus, we began our study by evaluating the amyloid-selectivity of the relaxation process from S_1(**dmAmide-H**) with the emitted fluorescence in the presence of $A\beta_{1\text{-}42}$ or other non-amyloid proteins/peptides. Our hypothesis for the amyloid-selective fluorescence emission is shown in Figure 2A. In the absence of amyloid, S_1(**dmAmide-H**) is supposed to decay through a non-radiation pathway with a twisted intramolecular charge transfer (TICT) state (S_1')[14] generated *via* bond rotation between the dimethylamino phenyl and pyrazine moieties. In the presence of amyloid, however, this bond rotation would be inhibited by interactions with amyloid, leading to fluorescence emission. Indeed, we observed chemiluminescence when **dmCLA-H** and Aβ amyloid coexisted (Figure 2B). The luminescence gradually decreased according to the time course accompanied by the conversion of **dmCLA-H** to **dmAmide-H**. The luminescence in the presence of monomer Aβ was likely due to amyloid formation during the measurement. There was no luminescence with other non-amyloid proteins (RNase A and lysozyme) and peptides (angiotensin IV and neurokinin A), showcasing the amyloid-selective chemiluminescence of **dmCLA-H**. **dmCLA-H** was also chemiluminescent with tau (Figure S1A) and αSyn (Figure S1B) amyloids, suggesting its general applicability to amyloids containing the cross-β sheet structure.

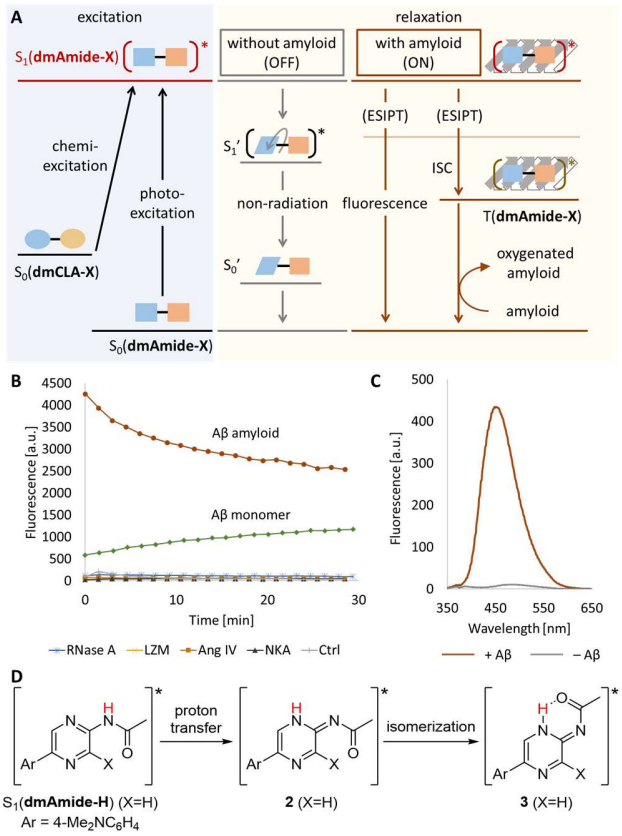

Figure 2. Photochemical pathways and luminescence properties of **dmCLA-X** and **dmAmide-X**. **A.** Overview of the photochemical pathways. **B.** Luminescence profiles of **dmCLA-H** (500 μM) in the presence of various peptides (20 μM) or proteins (90 μg/mL) in 0.1 M phosphate buffer (PB) (pH 7.4). Aβ amyloid: Aβ isopeptide[15] dissolved in 0.1 M PB and preincubated for 3 h. Aβ monomer: Aβ isopeptide dissolved in 0.1 M PB and used immediately. RNase A: ribonuclease A. LZM: lysozyme. Ang IV: angiotensin IV. NKA: neurokinin A. **C.** Fluorescence spectra of **dmAmide-H** (10 μM) with (+) or without (-) Aβ amyloid (10 μM). **D.** Reaction scheme of ESIPT from S_1(**dmAmide-H**).

To gain mechanistic insight into the relaxation process in the presence of amyloid, we next studied the fluorescence properties of **dmAmide-H**. The excited state [S_1(**dmAmide-H**)] is identical through chemiexcitation of **dmCLA-H** and photoexcitation of **dmAmide-H** (Figure 2A). The fluorescence of **dmAmide-H** was markedly enhanced by the presence of Aβ amyloid compared with its absence (Figure 2C), indicating the interaction between Aβ and **dmAmide-H** and modulation of the relaxation process. The presumed fluorescence mechanism involving the inhibition of the TICT pathway by interaction with amyloid was in part supported by the enhanced **dmCLA-H** fluorescence in viscous solutions composed of a glycerol-water mixture (Figure S2A). However, the maximum fluorescence wavelength differed between the two conditions: λ_{max} = 450 nm in the presence of Aβ amyloid (Figure 2C), whereas λ_{max} = 375 nm in 75% glycerol in water (Figure S2B). **dmAmide-H** exhibited a large Stokes shift in the presence of Aβ amyloid: the maximum wavelengths of absorption and fluorescence were 340 nm (Figure S3) and 450 nm (Figure 2C), respectively. This

suggests an alternative relaxation pathway from S_1(**dmAmide-H**) by the interaction with amyloid.

Based on theoretical studies, we attributed this photochemical property of **dmAmide-H** to an excited-state intramolecular proton-transfer (ESIPT)[16] process (Figures 2D, S4A, and S4B). In low-polar environments, which mimics the binding site in Aβ, S_1(**dmAmide-H**) decays through proton transfer and isomerization to afford **3** containing an intramolecular hydrogen bond, followed by fluorescence emission. The calculated fluorescence wavelength through ESIPT (434 nm) matched with the observed value (450 nm) (Figure S4B). In contrast, non-luminescent TICT pathway is favorable in water environments (Figures S4C and S4D). The dependency of the relaxation mechanism on the environmental polarity was also supported by solvatochromism of **dmAmide-H**; the fluorescence wavelength in dichloromethane (480 nm) was closer to that in the presence of Aβ amyloid (450 nm, Figure 2C) than that in water (370 nm, Figure S5). The fluorescence intensity was significantly greater in dichloromethane than in water. Thus, **dmAmide-H** fluoresces in the presence of Aβ amyloid by binding and inhibiting generation of the TICT state, as well as promoting the ESIPT pathway by sensing the hydrophobic environment of amyloid.[17]

We then developed compounds capable of selective Aβ oxygenation without photoirradiation, based on the **dmCLA-H** structure. Aiming at enhancing intersystem crossing (ISC) to generate an excited triplet state of **dmAmide-H** [T(**dmAmide-H**)] (Figure 2A), we synthesized **dmCLA-Cl** and **dmCLA-Br** containing the heavy atoms,[18] Cl and Br, respectively (Figure 1C). After oxygenation of Aβ [20 μM in 0.1 M PB (pH 7.4)] using **dmCLA-H**, **dmCLA-Cl**, or **dmCLA-Br** (500 μM, 37 °C for 24 h in the dark), oxygenation yield was evaluated by analyzing the oxygenated products with matrix assisted laser desorption/ionization time of flight mass spectrometry (MALDI TOF-MS) to be 19%, 26%, or 29% (Figure S6). Enzymatic digestion of the products and MS analysis of the peptide fragments revealed that the main oxygenated amino acid residue was ^{35}Met (Figures 3A and S7). Consistent with previous reports,[19] oxygenated Aβ furnished reduced amyloidogenic properties, as was represented by the reduced fluorescence with ThT (Figure S8). We also confirmed that **dmCLA-Cl** oxygenated αSyn and tau amyloids (Figures S9 and S10).

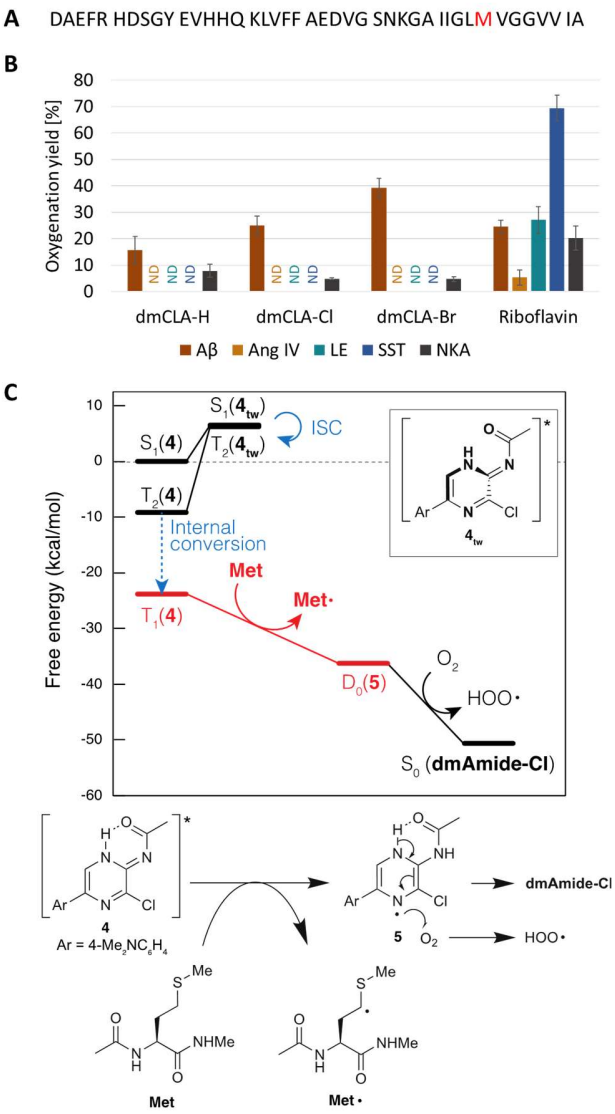

Figure 3. Amyloid-selective chemiexcited oxygenation with **dmCLA-X**. **A.** Amino acid sequence of $Aβ_{1-42}$. The oxygenation site Met is colored in red. **B.** Evaluation of amyloid selectivity. A mixture of Aβ, Ang IV, LE, SST, and NKA (4 μM each in 0.1 M PB) was incubated at 37 °C for 24 h, and oxygenation yield of each peptide was calculated by MALDI TOF-MS (ND: not detected). As a control, photooxygenation of the mixture with riboflavin (1 μM) was also conducted. The values are obtained by subtracting the oxygenation yield without the addition of **dmCLA-X.** Amino acid sequences of off-target model peptides; Ang IV: VYIHPF. LE: PyrEHWSYLLPR (Pyr: pyroglutamic acid). SST: AG*C*KNFFWKTFT*SC* (two *C*'s form an intramolecular disulfide bond). NKA: HKTDSFVGLM-NH_2. **C.** Energy diagram of the relaxation process in the presence of amyloids.

Subsequently, we evaluated the Aβ amyloid-selectivity of the chemiexcited oxygenation compared to non-amyloid off-target model peptides containing oxidation-sensitive amino acids residues, angiotensin IV (Ang IV), leuprorelin (LE), somatostatin (SST), and neurokinin A (NKA) (Figure 3B). Photooxygenation with riboflavin, a non-selective photosensitizer, resulted in the oxygenation of all the peptides. However, **dmCLA-X** furnished amyloid selectivity with **dmCLA-Br** as the most reactive and selective compound, producing a >8:1 selectivity of Aβ amyloid

vs. NKA. Oxygenation of Ang IV, LE, and SST were not detected. The amyloid selectivity is likely due to the above-described, amyloid-dependent relaxation pathway from S_1(**dmAmide-X**), generated by chemiexcitation of **dmCLA-X**.

On the basis of theoretical calculations, a plausible relaxation pathway from **4** is proposed in Figure 3C using **dmCLA-Cl** as a representative molecule. S_1(**4**) derived from **dmCLA-Cl** through chemiexcitation and ESIPT is first distorted along the imine C=N bond (**4**$_{tw}$). At the distorted state, energies of S_1 and T_2 states are almost degenerate, and the spin-orbit coupling (SOC) constant is non-zero, which enhances ISC between S_1(**4**$_{tw}$) and T_2(**4**$_{tw}$) states. After ISC and the internal conversion, **dmCLA-Cl** reaches T_1(**4**). The reaction between T_1(**4**) and Met affords the radical state D_0(**5**) and Met$^{\bullet}$, which acts as a precursor to sulfoxide.[20,21] The activation free energy of this Met$^{\bullet}$ generation step is approximately 12 kcal/mol, suggesting the facile progression of this step at room temperature (Figure S11). Electron transfer from D_0(**5**) to O_2 and subsequent proton transfer afford hydroperoxyl radical (HOO$^{\bullet}$) in equilibrium with superoxide ($O_2^{\bullet-}$) and S_0(**4**), which further isomerizes to afford **dmAmide-Cl** at the ground state.

The generation of $O_2^{\bullet-}$ was experimentally supported. Thus, a mixture of **dmCLA-Cl** (500 μM), Aβ (20 μM), and a ROS detector [nitro blue tetrazolium (NBT)[22] for $O_2^{\bullet-}$ or furfuryl alcohol (FFA)[23] for singlet oxygen ($^1O_2$); 500 μM] (Figure S12A) was incubated at 37 °C for 24 h, and the remaining detector was quantified by HPLC analysis. Consequently, while a 20% decrease of NBT and purple precipitate of formazan were observed using NBT, there was no detectable decrease of FFA (Figures S12B and S12C). Reactions using ROS scavengers (sodium L-ascorbate for superoxide and sodium azide for $^1O_2$)[24] also supported the generation of superoxide, but not $^1O_2$ (Figure S12D).

We also examined the origin of the oxygenation activity difference between three **dmCLA-X** (X = H, Cl, Br). The SOC value at ISC is significantly larger when X = Br than when X = H and Cl, leading to faster ISC (Figures S13). This rationalizes the high oxygenation activity of **dmCLA-Br**. However, differences in the SOC value and the activation energy for the Met oxidation step (Figure S11) between X = H and Cl are small and cannot explain the reactivity difference between **dmCLA-H** and **dmCLA-Cl**. Therefore, we searched for parameters to dictate the difference and found that the binding affinity to amyloid may be critical.[25] Dissociation constant (K_d) of **dmCLA-Cl** (K_d = 0.72 μM) was significantly smaller than **dmCLA-H** (K_d = 5.0 μM) (Table S1), suggesting that **dmCLA-Cl** binds more strongly to amyloids than **dmCLA-H**.

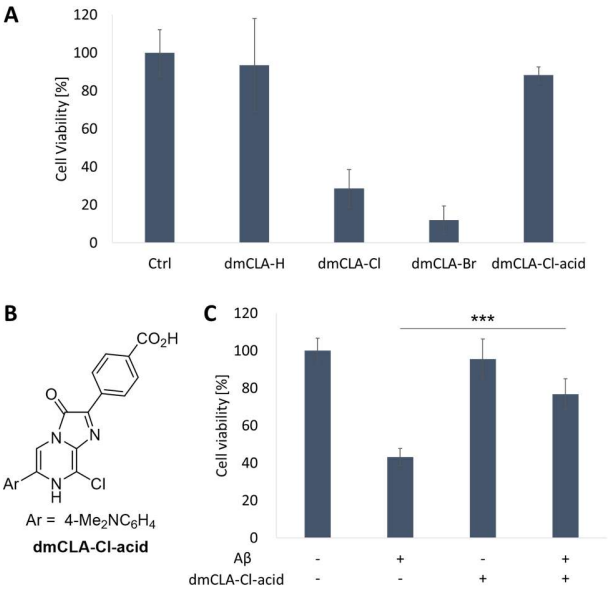

Figure 4. Cell viability assays of **dmCLA-X** and **dmCLA-Cl-acid**. **A.** PC12 cell viability after incubation with **dmCLA-H**, **-Cl**, **-Br**, or **-Cl-acid** (25 μM) in DMEM at 37 °C for 2 days. Data are averages of six experimental runs. Error bars indicate standard deviation. **B.** Structure of **dmCLA-Cl-acid**. **C.** PC12 cell viability after incubation with Aβ (5 μM) and **dmCLA-Cl-acid** (25 μM) in DMEM at 37 °C for 2 days. Data are averages of six experimental runs. Error bars indicate standard deviation (*** $P < 0.001$ by Tukey's test).

Finally, we studied the effects of Aβ amyloid oxygenation by **dmCLA-X** in the experiments using PC12 cells (Figure 4). In the absence of Aβ, however, the three **dmCLA-X**, especially **dmCLA-Cl** and **-Br** were cytotoxic by themselves under the conditions where Aβ was sufficiently oxygenated (Figure 4A). **dmCLA-Cl** demonstrated lower toxicity than **dmCLA-Br**. Therefore, to reduce the toxicity, we started by modifying the structure of **dmCLA-Cl**. We synthesized **dmCLA-Cl-acid** by introducing a carboxylic acid group to prevent cell penetration and enhance water solubility (Figure 4B). As expected, **dmCLA-Cl-acid** showed much lower toxicity (LC_{50} = 50 μM) without diminishing oxygenation reactivity to amyloid (18% yield under the conditions of Figure 3B). Using **dmCLA-Cl-acid**, we performed a live cell rescue assay in the presence of Aβ amyloid (Figure 4C). Aβ alone decreased the cell viability to ca. 40%, whereas the cell viability increased to approximately 80% in the presence of **dmCLA-Cl-acid**. This result demonstrated that **dmCLA-Cl-acid** reduced toxicity of Aβ amyloid through selective oxygenation in the presence of living cells without relying on photoirradiation.

In summary, we developed the unimolecular chemiexcited oxygenation of amyloids based on *Cypridina* luciferin analogs **dmCLA-Cl**, **-Br**, and **-Cl-acid**. The ability to proceed without photoirradiation is the principal advantage of this approach over the previous photooxygenation method. Due to the amyloid-specific relaxation process from the chemiexcited state involving ESIPT and ISC, the oxygenation reaction targeted and neutralized amyloids even in the presence of off-targets and in experiments using cells. This unimolecular system is simpler than the previous bimolecular system using CRET,[9] and thus might have a potential for more straightforward clinical

applications in the future. Further studies toward *in vivo* applications are ongoing.

ASSOCIATED CONTENT

Supporting Information

The Supporting Information is available free of charge on the ACS Publications website. Synthetic protocols, experimental details, Figure S1-S16, and Table S1 (PDF).

AUTHOR INFORMATION

Corresponding Author

Motomu Kanai – Laboratory of Synthetic Organic Chemistry, Graduate School of Pharmaceutical Sciences, The University of Tokyo, 7-3-1 Hongo, Bunkyo-ku, Tokyo, 113-0033, Japan; orcid.org/0000-0003-1977-7648; Email: kanai@mol.f.u-tokyo.ac.jp

Authors

Hiroki Umeda – Laboratory of Synthetic Organic Chemistry, Graduate School of Pharmaceutical Sciences, The University of Tokyo, 7-3-1 Hongo, Bunkyo-ku, Tokyo, 113-0033, Japan

Kayo Suda – Laboratory of Theoretical Chemistry, Graduate School of Arts and Sciences, The University of Tokyo, Tokyo 153-8902, Japan

Daisuke Yokokawa – Laboratory of Theoretical Chemistry, Graduate School of Arts and Sciences, The University of Tokyo, Tokyo 153-8902, Japan

Shigehiro A. Kawashima – Laboratory of Synthetic Organic Chemistry, Graduate School of Pharmaceutical Sciences, The University of Tokyo, 7-3-1 Hongo, Bunkyo-ku, Tokyo, 113-0033, Japan

Harunobu Mitsunuma – Laboratory of Synthetic Organic Chemistry, Graduate School of Pharmaceutical Sciences, The University of Tokyo, 7-3-1 Hongo, Bunkyo-ku, Tokyo, 113-0033, Japan and JST, PRESTO, 4-1-8 Honcho, Kawaguchi, Saitama 332-0012, Japan

Yuki Yamanashi – Laboratory of Synthetic Organic Chemistry, Graduate School of Pharmaceutical Sciences, The University of Tokyo, 7-3-1 Hongo, Bunkyo-ku, Tokyo, 113-0033, Japan

Notes

The authors declare no competing financial interest.

ACKNOWLEDGMENT

This research was supported by JSPS KAKENHI grant numbers JP23H04909 (Green Catalysis Science) and JP23H05466 (M.K.), JP20H05843 (Dynamic Exciton) (H.M.), and JP23H04911 (Green Catalysis Science) and JST-PRESTO grant number JPMJPR21C9 (D.Y.). We thank Professor Shojiro Maki and Dr. Nobuo Kitada in The University of Electro-Communications for valuable suggestions.

REFERENCES

(1) (a) Iadanza, M. G.; Jackson, M. P.; Hewitt, E. W.; Ranson, N. A.; Radford, S. E. A New Era for Understanding Amyloid Structures and Disease. *Nat. Rev. Mol. Cell. Biol.* **2018**, *19*, 755–773. (b) Ke, P. C.; Zhou, R.; Serpell, L. C.; Riek, R.; Knowles, T. P. J.; Lashuel, H. A.; Gazit, E.; Hamley, I. W.; Davis, T. P.; Fändrich, M.; Otzen, D. E.; Chapman, M. R.; Dobson, C. M.; Eisenberg, D. S.; Mezzenga, R. Half a Century of Amyloids: Past, Present and Future. *Chem. Soc. Rev.* **2020**, *49*, 5473–5509.

(2) van Dyck, C. H.; Swanson, C. J.; Aisen, P.; Bateman, R. J.; Chen, C.; Gee, M.; Kanekiyo, M.; Li, D.; Reyderman, L.; Cohen, S.; Froelich, L.; Katayama, S.; Sabbagh, M.; Vellas, B.; Watson, D.; Dhadda, S.; Irizarry, M.; Kramer, L. D.; Iwatsubo, T. Lecanemab in Early Alzheimer's Disease. *N. Engl. J. Med.* **2023**, *388*, 9–21.

(3) Kanai, M.; Takeuchi, Y. Catalysis Medicine: Participating in the Chemical Networks of Living Organisms through Catalysts. *Tetrahedron* **2023**, *131*, 133227.

(4) Sohma, Y.; Sawazaki, T.; Kanai, M. Chemical Catalyst-Promoted Photooxygenation of Amyloid Proteins. *Org. Biomol. Chem.* **2021**, *19*, 10017–10029.

(5) For representative chemical modifications of amyloids other than photooxygenation, see: (a) Derrick, J. S.; Lee, J.; Lee, S. J. C.; Kim, Y.; Nam, E.; Tak, H.; Kang, J.; Lee, M.; Kim, S. H.; Park, K.; Cho, J.; Lim, M. H. Mechanistic Insights into Tunable Metal-Mediated Hydrolysis of Amyloid-β Peptides. *J. Am. Chem. Soc.* **2017**, *139*, 2234–2244. (b) Han, J.; Lee, H. J.; Kim, K. Y.; Nam, G.; Chae, J.; Lim, M. H. Mechanistic Approaches for Chemically Modifying the Coordination Sphere of Copper–Amyloid-β Complexes. *Proc. Natl. Acad. Sci.* **2020**, *117*, 5160–5167. (c) Gao, N.; Liu, Z.; Zhang, H.; Liu, C.; Yu, D.; Ren, J.; Qu, X. Site-Directed Chemical Modification of Amyloid by Polyoxometalates for Inhibition of Protein Misfolding and Aggregation. *Angew. Chem. Int. Ed.* **2022**, *61*, e202115336.

(6) Nagashima, N.; Ozawa, S.; Furuta, M.; Oi, M.; Hori, Y.; Tomita, T.; Sohma, Y.; Kanai, M. Catalytic Photooxygenation Degrades Brain Aβ in Vivo. *Sci. Adv.* **2021**, *7*, eabc9750.

(7) Even highly tissue-penetrating near-infrared light (λ = 808 nm) is estimated to reach 4 cm depth into the body. See; Tedford, C. E.; DeLapp, S.; Jacques, S.; Anders, J. Quantitative Analysis of Transcranial and Intraparenchymal Light Penetration in Human Cadaver Brain Tissue. *Lasers Surg. Med.* **2015**, *47*, 312–322.

(8) (a) Yang, J.; Yin, W.; Van, R.; Yin, K.; Wang, P.; Zheng, C.; Zhu, B.; Ran, K.; Zhang, C.; Kumar, M.; Shao, Y.; Ran, C. Turn-on Chemiluminescence Probes and Dual-Amplification of Signal for Detection of Amyloid Beta Species in Vivo. *Nat. Commun.* **2020**, *11*, 4052. (b) Zhang, J.; Wickizer, C.; Ding, W.; Van, R.; Yang, L.; Zhu, B.; Yang, J.; Wang, Y.; Wang, Y.; Xu, Y.; Zhang, C.; Shen, S.; Wang, C.; Shao, Y.; Ran, C. In Vivo Three-Dimensional Brain Imaging with Chemiluminescence Probes in Alzheimer's Disease Models. *Proc. Natl. Acad. Sci.* **2023**, *120*. (c) Ran, C.; Pu, K. Molecularly generated light and its biomedical applications. *Angew. Chem. Int. Ed.* **2023**, *63*, e202314468.

(9) Kuang, S.; Zhu, B.; Zhang, J.; Yang, F.; Wu, B.; Ding, W.; Yang, L.; Shen, S.; Liang, S. H.; Mondal, P.; Kumar, M.; Tanzi, R. E.; Zhang, C.; Chao, H.; Ran, C. A Photolabile Curcumin-Diazirine Analogue Enables Phototherapy with Physically and Molecularly Produced Light for Alzheimer's Disease Treatment. *Angew. Chem. Int. Ed.* **2023**, *62*, e202312519.

(10) da Silva *et al.* reported a unimolecular chemiluminescent photodynamic therapy exhibiting cytotoxicity to cancer cells: da Silva, L. P.; Núnez-Montenegro, A.; Magalhães, C. M.; Ferreira, P. J. O.; Duarte, D.; González-Berdullas, P.; Rodríguez-Borges, J. E.; Vale, N.; da Silva, J. C. G. E. Single-Molecule Chemiluminescent Photosensitizer for a Self-Activating and Tumor-Selective Photodynamic Therapy of Cancer. *Eur. J. Med. Chem.* **2019**, *183*, 111683. Our work, however, oxygenates amyloid molecules selectively without exhibiting cytotoxicity by tuning the catalyst structure.

(11) Ozawa, S.; Hori, Y.; Shimizu, Y.; Taniguchi, A.; Suzuki, T.; Wang, W.; Chiu, Y. W.; Koike, R.; Yokoshima, S.; Fukuyama, T.; Takatori, S.; Sohma, Y.; Kanai, M.; Tomita, T. Photo-Oxygenation by a Biocompatible Catalyst Reduces Amyloid-β Levels in Alzheimer's Disease Mice. *Brain* **2021**, *144*, 1884–1897.

(12) Hirano, T.; Takahashi, Y.; Kondo, H.; Maki, S.; Kojima, S.; Ikeda, H.; Niwa, H. The Reaction Mechanism for the High Quantum Yield of Cypridina (Vargula) Bioluminescence Supported by the Chemiluminescence of 6-Aryl-2-Methylimidazo[1,2-a]Pyrazin-3(7H)-Ones (Cypridina Luciferin Analogues). *Photochem. Photobiol. Sci.* **2008**, *7*, 197–207.

(13) Amdursky, N.; Erez, Y.; Huppert, D. Molecular Rotors: What Lies Behind the High Sensitivity of the Thioflavin-T Fluorescent Marker. *Acc. Chem. Res.* **2012**, *45*, 1548–1557.
(14) Wang, C.; Chi, W.; Qiao, Q.; Tan, D.; Xu, Z.; Liu, X. Twisted Intramolecular Charge Transfer (TICT) and Twists beyond TICT: From Mechanisms to Rational Designs of Bright and Sensitive Fluorophores. *Chem. Soc. Rev.* **2021**, *50*, 12656–12678.
(15) Sohma, Y.; Hayashi, Y.; Kimura, M.; Chiyomori, Y.; Taniguchi, A.; Sasaki, M.; Kimura, T.; Kiso, Y. The 'O-Acyl Isopeptide Method' for the Synthesis of Difficult Sequence-Containing Peptides: Application to the Synthesis of Alzheimer's Disease-Related Amyloid β Peptide (Aβ) 1-42. *J. Pept. Sci.* **2005**, *11*, 441–451.
(16) Hong, M.; Kim, M.; Yoon, J.; Lee, S.-H.; Baik, M.-H.; Lim, M. H. Excited-State Intramolecular Hydrogen Transfer of Compact Molecules Controls Amyloid Aggregation Profiles. *JACS Au* **2022**, *2*, 2001-2012.
(17) Kim, S.; Lee, H. J.; Nam, E.; Jeong, D.; Cho, J.; Lim, M. H.; You, Y. Tailoring Hydrophobic Interactions between Probes and Amyloid-β Peptides for Fluorescent Monitoring of Amyloid-β Aggregation. *ACS Omega* **2018**, *3*, 5141–5154.
(18) Solov'ev, K. N.; Borisevich, E. A. Intramolecular Heavy-Atom Effect in the Photophysics of Organic Molecules. *Phys.-Uspekhi* **2005**, *48*, 231–253.
(19) Hou, L.; Kang, I.; Marchant, R. E.; Zagorski, M. G. Methionine 35 Oxidation Reduces Fibril Assembly of the Amyloid Aβ-(1–42) Peptide of Alzheimer's Disease. *J. Biol. Chem.* **2002**, *277*, 40173–40176.
(20) Grassi, L.; Cabrele, C. Susceptibility of Protein Therapeutics to Spontaneous Chemical Modifications by Oxidation, Cyclization, and Elimination Reactions. *Amino Acids* **2019**, *51*, 1409–1431.
(21) The Met-selective modification with photoactivated compounds was reported. See; Kim, J.; Li, B. X.; Huang, R. Y.-C.; Qiao, J. X.; Ewing, W. R.; MacMillan, D. W. C. Site-Selective Functionalization of Methionine Residues via Photoredox Catalysis. *J. Am. Chem. Soc.* **2020**, *142*, 21260-21266. In this paper, selectivity is explained by the reactivity of Met•.
(22) Bielski, B. H. J.; Shiue, G. G.; Bajuk, S. Reduction of nitro blue tetrazolium by CO2- and O2- radicals. *J. Phys. Chem.* **1980**, *84*, 830-833.
(23) Haag, W. R.; Hoigne´, J.; Gassman, E.; Braun, A. Singlet Oxygen in Surface Waters — Part I: Furfuryl Alcohol as a Trapping Agent. *Chemosphere* **1984**, *13*, 631–640.
(24) Chen, W.; Wang, Z.; Tian, M.; Hong, G.; Wu, Y.; Sui, M.; Chen, M.; An, J.; Song, F.; Peng, X. Integration of TADF Photosensitizer as "Electron Pump" and BSA as "Electron Reservoir" for Boosting Type I Photodynamic Therapy. *J. Am. Chem. Soc.* **2023**, *145*, 8130–8140.
(25) The higher reactivity of **dmCLA-Cl** than **dmCLA-H** is also likely due to the difference in conversion efficiency to S_1 state in the chemiexcitation process. This is evidenced by the observed stronger luminescence of **dmCLA-Cl** than **dmCLA-H** (Figure S14) despite the comparable oscillator strength (f = 0.2021 for **dmCLA-H** and f = 0.2291 for **dmCLA-Cl**: Table S15) and SOC (Figure S12). The higher efficiency in generating S_1 for **dmCLA-Cl** leads to higher conversion efficiency to T_1, active species for oxygenation.